Journal of Inorganic Biochemistry 104 (2010) 1195–1204

Contents lists available at ScienceDirect

Journal of Inorganic Biochemistry

journal homepage: www.elsevier.com/locate/jinorgbio

Zinc(II) tweezers containing artificial peptides mimicking the active site of *phosphotriesterase*: The catalyzed hydrolysis of the toxic organophosphate parathion

Mohamed M. Ibrahim [a,c,*], Gaber A.M. Mersal [b,c]

[a] Chemistry Department, Faculty of Science, Kafr El-Sheikh University, Kafr El-Sheikh 33516, Egypt
[b] Chemistry Department, Faculty of Science, South Valley University, Qena, Egypt
[c] Chemistry Department, Faculty of Science, Taif University, 888 Hawaiya, Saudi Arabia

ARTICLE INFO

Article history:
Received 19 May 2010
Received in revised form 14 July 2010
Accepted 15 July 2010
Available online 23 July 2010

Keywords:
Syntheses
Artificial peptides
Trinuclear zinc(II) complex
Modeling
Parathion
Detoxification

ABSTRACT

Two new ligand-containing histidine based on *N,N′,N″*-tris(N-benzyl-L-histidinyl)tri(2-aminoethyl)amine, **L^1**, namely *N,N′,N″*-tris[(1S)-2-methoxy-2-oxy-1-(1-benzylimidazol-4-ylmethyl)]nitrilotriacetamide **L^2** and *N,N′,N″*-tris{N-benzyl-N-[N-benzyl-N-(N-benzyl-L-histidinyl)-L-histidinyl]-L-histidinyl}tri(2-aminoethyl) amine **L^3** were prepared. Zinc(II) binding studies by these ligand systems were analyzed by means of potentiometric and ^{1}H NMR titrations in aqueous methanol (33 % *v/v*). Subsequently their zinc(II) complexes [**L^1**Zn(H_2O)](ClO_4)$_2$·$HClO_4$ (**1**), [**L^2**Zn(OH_2)](ClO_4)$_2$·H_2O (**2**), and ([**L^3**Zn_3(H_2O)$_3$](ClO_4)$_6$·3$HClO_4$·5H_2O (**3**), respectively were synthesized and characterized. The reactivity of the trinuclear complex (**3**) toward the hydrolysis of the toxic organophosphate parathion was investigated and compared with that of the mononuclear reference complex (**1**). From the pH dependence of the apparent rate constants, and the deprotonation constant (pK_a) of the coordinated water molecules in (**1**), the active species were confirmed to be {[H**L^1**Zn(OH)]$^{2+}$/[**L^1**Zn(H_2O)]$^{2+}$} at pH 8.5. The trizinc complex (**3**) effects hydrolysis of parathion, with three times rate enhancement over the mononuclear (**1**), indicating that cooperative action of the three zinc centers is limited.

1. Introduction

The development of metal-containing catalysts for the rapid hydrolysis of toxic organophosphorus triesters is of fundamental and practical interest since these compounds appear from day-to-day applications as pesticides and potent chemical warfare agents [1,2]. Several hydrolytic enzymes in nature, including *phosphatases* [3–5], often possess two (or more) metal ions at their active sites. These metal ions, and/or the water bound to them, cooperate and as a result, hydrolyze stable phosphoesters under physiological conditions [6–23]. The presence of two or three zinc(II) centers in a single complex appears to be important for activation and recognition of cleavage sites within phosphate esters [24–28]. Moreover, these complexes generate highly cationic species that favor the electrostatic attraction to the phosphate backbone.

The search for simple, yet effective, synthetic metal containing catalysts which mimic metalloenzymes and may exploit their synergistic effects, is a significant goal in chemistry [29–32]. Several studies have been devoted to elucidate the effect of the ligand structure in modulating the reactivity of the metal center [33–36] but it is quite clear that the desired acceleration cannot be reached with simple mononuclear complexes [37–44].

Recently, in order to increase the reactivity of artificial hydrolytic catalysts, several hydrolytic metalloenzyme models containing di- and trinuclear zinc(II) complexes have been designed and studied to account for or mimic the function played by the cooperativity of two or three zinc(II) ions, as occurs in several *phosphatases* and *nucleases* [45–59]. In these systems, we found that the multinuclear complexes were generally more active than their corresponding mononuclear ones. This inspired us to probe further into how molecular level effects with respect to the structure of the ligand and the overall nature of the bi- and trimetallic coordination complex affect the activity of the catalyst system.

In our recent studies, we have investigated the mononuclear zinc (II) complex (**1**), derived from the trihistidine, *N,N′,N″*-tris(N-benzyl-L-histidinyl)tri(2-aminoethyl)amine **L^1** as a catalyst in the cleavage of phosphate diester bis(*p*-nitrophenyl)phosphate ($BNPP^-$) [60]. The higher efficiency of (**1**) arises from the lowering the pK_a value of Zn (II)-bound water molecule. It is important to elucidate the cooperation effect of three zinc(II) ions in phosphoester hydrolysis, since three zinc ions have been suggested to participate in enzymatic reactions [61–64]. Thus, one of the objectives of the present work is to modify the structure of the histidine ligand **L^1** [60] and change the metal-to-ligand ratio. The source of this high reactivity is the ability of

* Corresponding author. Chemistry Department, Faculty of Science, Taif University, 888 Taif, Saudi Arabia.
E-mail address: ibrahim652001@yahoo.com (M.M. Ibrahim).

0162-0134/$ – see front matter © 2010 Elsevier Inc. All rights reserved.
doi:10.1016/j.jinorgbio.2010.07.009

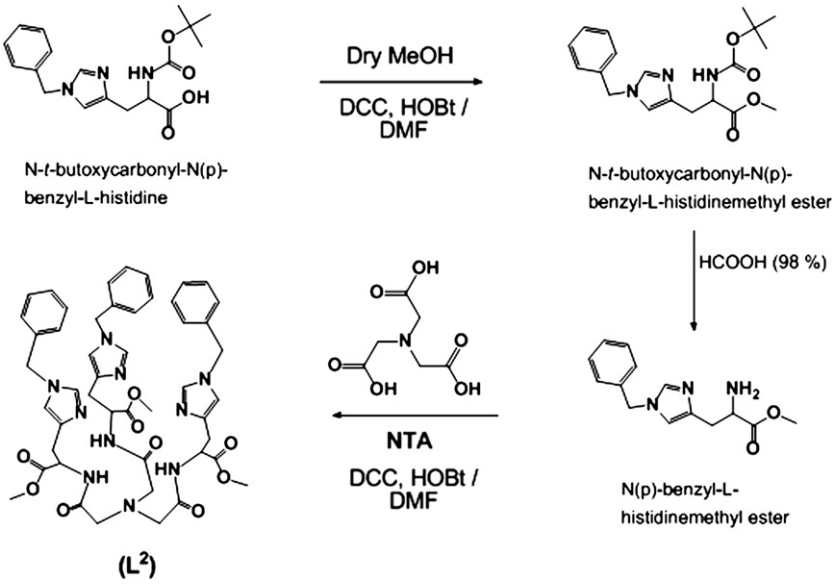

Scheme 1. The synthesis of ligand tris(Im-bzl-L-histiylmethylestermethyl)amine (**L²**).

the complex to activate the phosphate ester toward the nucleophilic attack using the triple zinc(II) activation and their cooperativities.

As part of our studies in biomimetic hydrolytic zinc enzymes [39–45,60] and with the aim to mimic the key features of the three zinc(II) centers in these metalloenzymes, we designed and synthesized two new ligands containing artificial tri and nonapeptide, namely *N*,*N*′,*N*″-tris[(1S)-2-methoxy-2-oxy-1-(1-benzylimidazol-4-ylmethyl)]nitrilotriacetamide **L²** (Scheme 1) and *N*,*N*′,*N*″-tris{N-benzyl-N-[N-benzyl-N-(N-benzyl-L-histidinyl)-L-histidinyl]-L-histidinyl}tri(2-aminoethyl)amine **L³** (Scheme 2) and their zinc(II) complexes (Scheme 3) by affixing histidine coordination sites with bulky substituents on the periphery of nitrilotriacetic acid (NTA) and tris(2-aminoethyl)amine (TREN), respectively. The protonation constants (pK_a) values of the ligands as well as the stability constants ($\log K_{st}$) and deprotonation equilibria (pK_a (H_2O)) of their zinc complexes are reported. Further information about zinc complexes of the ligands is obtained from R ($=[Zn^{2+}]_o/[L]_o$)-dependent ^1H NMR titrations. To assess the degree of synergism between zinc(II) ions in the trinuclear complex (**3**), its catalytic

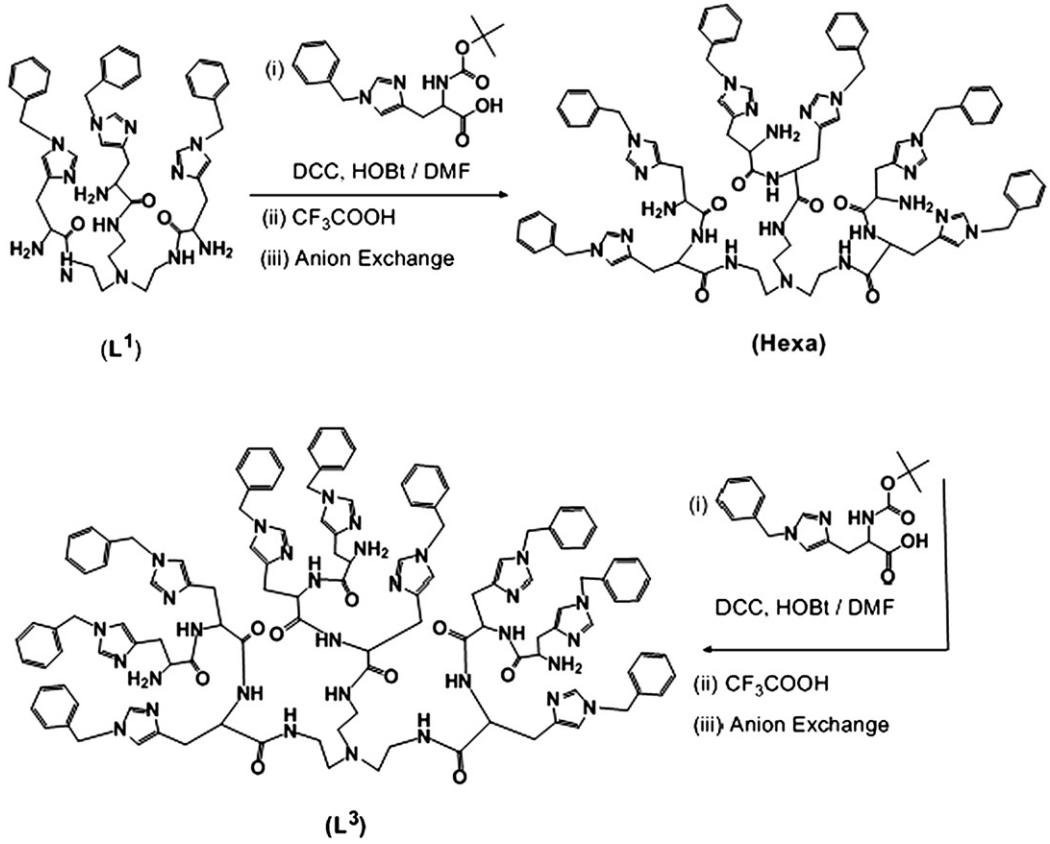

Scheme 2. The synthesis of the artificial peptide tris{[tris(benzyl-im-histidyl-aminoethyl}amine (**L³**).

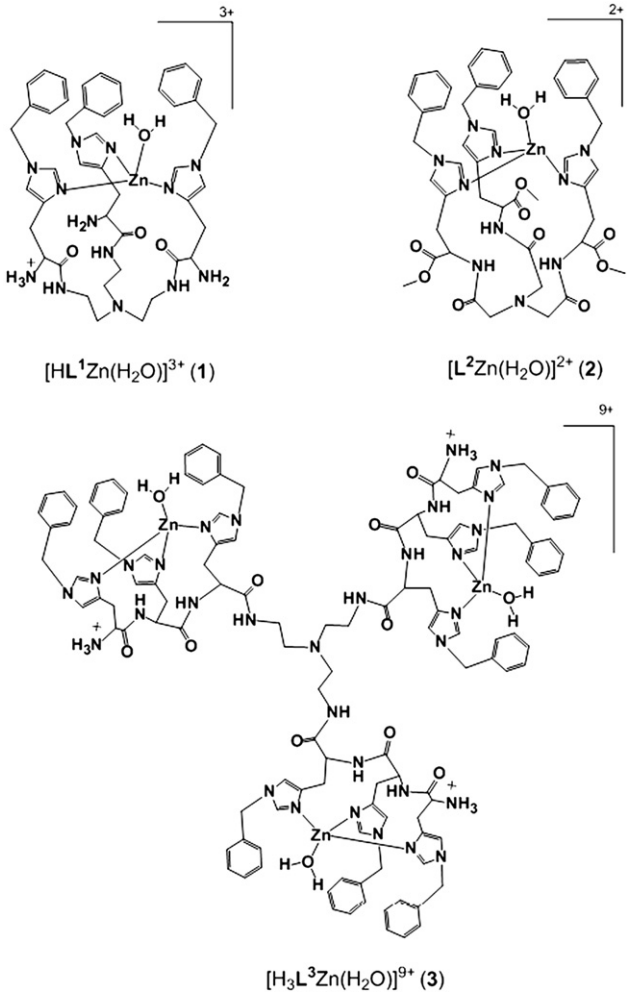

Scheme 3. The proposed structures of zinc(II) complexes (**1**), (**2**), and (**3**).

efficiency towards the hydrolysis of the toxic organophosphate parathion (DENTP) (Scheme 4) was compared with the monomeric analogue (**1**). These results obtained, in turn, were able to provide certain clues to the nature of the mechanism of action of this new trizinc nonahistidine complex.

2. Experimental

Caution: perchlorate salts of amine ligands and their metal complexes are potentially explosive and should be handled in small quantities.

2.1. Materials

All reagents and solvents used were of analytical grade. N(α)-(t-butoxycarbonyl-N(π)-benzyl-L-histidine and the organophosphate parathion were purchased from Sigma. The ligand *N*,*N*′,*N*″-tris(N-benzyl-L-histidinyl)tri(2-aminoethyl)amine $\mathbf{L^1}$ and its aqua zinc complex (**1**) were prepared as previously described [60].

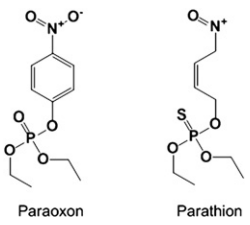

Scheme 4. The toxic organophosphates.

2.2. Syntheses

A frequent problem with the elemental analyses of tris(Im-bzl-L-histiylmethylester-methyl)amine $\mathbf{L^2}$ is that the carbon values are outside the accepted range. When this was the case here, at least one additional analysis value (FAB^+-Ms) was determined.

2.2.1. Synthesis of Im-bzl-L-histidine methyl ester *I*

Dry MeOH (83 mL, 2.60 mmol) was added to an ice-cold solution of dicyclohexylcarbodiimide (DCC, 0.59 g, 2.85 mmol), 1-hydroxybenzotriazole (HOBt, 0.40 g, 2.60 mmol) and N(α)-(t-butoxycarbonyl-N(π)-benzyl-L-histidine (0.89 g, 2.60 mmol) in dimethylformide (DMF, 5 mL). pH was adjusted to 7.0 by N-methylmorpholine (NMM). The reaction mixture was stirred at 0 °C for 2 h and at room temperature for 12 h, filtered, and evaporated to solidify which was suspended in dichloromethane (30 ml), extracted with 10% sodium carbonate (10 mL), dried which was dissolved in ethylacetate (EtOAc, 5 mL) and set aside at 4 °C overnight. Further dicyclohexylurea (DCU) was then filtered off and solvent was evaporated to give a hygroscopic powder. Yield: 0.90 g (96%) of Boc-**I**. ^{1}H NMR ($CDCl_3$, s = singlet, m = multiplet, br = broad): 7.36 (s, 1H; im *2′*), 7.30–7.22 (m, 3H, H-*b*,*c*), 7.05–7.03 (m, 2H, H-*a*), 6.58 (s, 1H; im *5′*), 5.83 (br, s, 1H, amide-NH), 4.93 (s, 2H, $-C^{\alpha}H_2$), 4.49–4.44 (m, 1H, His-$C^{\beta}H$) 3.57 (s, 3H, OCH_3), 3.02–2.93 (m, 2H, His-$C^{\gamma}H_2$), 1.34 (s, 9H, BOC). FAB^+-MS: *m*/*z*: 359 $[M+H]^+$.

To BOC-**I** (0.90 g, 2.51 mmol), formic acid (5 mL, 98%) was added; the removal of BOC group was monitored by TLC. After 15 h the formic acid was removed in vacuo. The residue was taken in water (10 ml) and washed with EtOAc (4×15 mL). The pH was then adjusted to 8 with solid sodium bicarbonate and extracted with EtOAc (3×20 ml). The extracts were pooled, washed with saturated brine, dried over sodium sulphate, and concentrated to dryness. Yield: 0.46 g (72%). ^{1}H NMR ($CDCl_3$, s = singlet, m = multiplet): 7.48 (s, 1H; im *2′*), 7.39–7.27 (m, 3H, H-*b*,*c*), 7.11–7.09 (m, 2H, H-*a*), 6.66 (s, 1H; im *5′*), 5.04 (s, 2H, $-C^{\alpha}H_2$), 4.90–4.86 (m, 1H, His-$C^{\beta}H$), 3.64 (s, 3H, OCH_3), 3.13–3.10 (m, 2H, His-$C^{\gamma}H_2$).

2.2.2. Synthesis of tris(Im-bzl-L-histiylmethylestermethyl)amine L^2

Nitrilotriacetic acid, NTA (0.17 g, 0.3 mmol) was added to an ice cold solution of dicyclohexylcarbodiimide (DCC) (0.12 g, 0.57 mmol), hydroxybenzotriazole (HOBt) (0.80 g, 0.51 mmol), and histidine methyl ester *I* (0.233 g, 0.09 mmol) in DMF (8 mL) and the pH was adjusted to 7 using *N*-methyl morpholine (NMM). The reaction mixture was stirred at 0 °C for 2 h and at room temperature for 12 h, filtered and evaporated to produce a solid which was suspended in CH_2Cl_2 (30 mL), extracted with 10% aqueous sodium carbonate (10 mL) and dried. The remaining solid was dissolved in EtOAc (5 mL) and kept at 4 °C overnight. Dicyclohexylurea (DCU) was then filtered off and the solvent was evaporated to give a white powder. Yield: 0.71 g, 83%. Anal. Calcd. for $C_{48}H_{54}N_{10}O_9\cdot 2H_2O$ (985.92 + 36.04): C, 60.62; H, 6.15; N, 14.73. Found: C, 59.39; H, 6.21; N, 14.57. ^{1}H NMR (CD_3OD:D_2O, 3:1, s = singlet, m = multiplet): 7.71 (s, 3H; im *2′*), 7.44–7.37 (m, 9H; H-*b*,*c*), 7.27–7.23 (m, 6H; H-*a*), 6.94 (s, 3H; im *5′*), 5.21 (s, 6H; $-C^{\alpha}H_2$), 4.81–4.79 (m, 3H; His-$C^{\beta}H$), 3.58 (s, 9H; OCH_3), 3.47 (s, 6H; N-CH_2), 3.13–3.07 (m, 6H; His-$C^{\gamma}H_2$). FAB^+-MS: *m*/*z*: 915 $[M+H]^+$, 825, 673, 628, 434, 272, 200, 91, and 81.

2.2.3. Synthesis of tris{[bis(benzyl-im-histidyl)aminoethyl}amine ***Hexa***

$\mathbf{L^1}$ (0.538 g, 0.65 mmol) was added to an ice-cold solution of DCC (0.44 g, 2.1 mmol), HOBt (0.30 g, 1.95 mmol), and N(α)-(t-butoxycarbonyl-N(π)-benzyl-L-histidine (0.64 g, 1.95 mmol) in DMF (8 mL). The pH was adjusted to 7.0 by addition of NMM. The reaction mixture was stirred at 0 °C ice-bath for 2 h, and after at room temperature for 15 h, filtered from the formed dicyclohexyl urea

(DCU), the solvent removed in vacuo to give a sticky solid material which was suspended in dichloromethane (30 mL), extracted with 10% Na_2CO_3. The organic phase was collected and dried on Na_2SO_4. The filtered clear solution was dried up, and redissolved in ethyl acetate (EtOAc, 5 mL) and was kept at 4 °C overnight. Further DCU was then filtered off, and the solvent was evaporated in vacuo to give a hygroscopic powder of Boc-**Hexa**. Yield: 0.69 g, 59%. Yield: 0.93 g, 79%. Anal. Calc. for $C_{99}H_{120}N_{22}O_{12}$ (1810.18): C, 65.69; H, 6.68; N, 17.02. Found: C, 64.17; H, 7.06; N, 17.57. ^{1}H NMR (400 MHz, $CDCl_3$, s = singlet, m = multiplet, br = broad): 7.50 (s, 6H, im *2′*), 7.33–7.25 (m, 18H, H-*b*,*c*), 7.24–7.20 (m, 12H, H-*a*), 6.82 (s, 6H, im *5′*), 5.90 (br, 6H, amide-NH), 5.22 (s, $-C^{\alpha}H_2$, 12H), 4.84 (m, 6H, His-$C^{\beta}H$), 3.35–3.22 (m, 6H, $-C^{\delta}H_2$), 3.08–3.03 (m, 12H, His-$C^{\gamma}H_2$), 2.86–2.83 (m, 6H, $^{-}C^{\sigma}H_2$), 1.33 (s, BOC, 54H).

Boc-**Hexa** (0.69 g) was dissolved in trifluoroacetic acid, TFA (5 mL) and stirred for 0.5 h at room temperature, then TFA was removed in vacuo. The remaining sticky material was dissolved in 10 mL water and was extracted with 30 mL ethyl acetate. The aqueous phase was collected which was then dried to obtain a hygroscopic powder of the acidic form of Hexa-TFA. Yield: 0.72 g, 68%. Anal. Calc. for $C_{84}H_{96}N_{22}O_6\cdot 10CF_3COOH\cdot 8H_2O$ (1509.8 + 1140.2 + 144): C, 44.70; H, 4.40; N, 11.03. Found: C, 44.90; H, 4.12; N, 10.53. ^{1}H NMR (400 MHz, D_2O, s = singlet, m = multiplet: 8.79 (s, 6H, im *2′*), 7.48–7.37 (m, 18H, H-*b*,*c*), 7.35–7.30 (m, 12H, H-*a*), 7.27 (s, 6H, im *5′*), 5.35 (s, 12H, $-C^{\alpha}H_2$), 4.56 (m, 6H, His-$C^{\beta}H$), 4.42 –4.37 (m, 6H, $-C^{\delta}H_2$), 3.49 (m, 6H, $-C^{\sigma}H_2$), 3.18–3.05 (m, 12H, His-$C^{\gamma}H_2$).

Hexa-TFA (0.70 g, 0.25 mmol) was passed through the anion-exchange column (Dowex, OH-form) according to a procedure described earlier for the synthesis of Hexa. Yield: 0.18 g, 53%. Anal. Calc. for $C_{84}H_{96}N_{22}O_6\cdot 3H_2O$ (1509.83 + 54.05): C, 64.51; H 6.57; N, 19.70. Found: C, 64.99; H, 6.83; N, 19.24. ^{1}H NMR (400 MHz, D_2O, s = singlet, m = multiplet): 7.63 (s, 6H, im *2′*), 7.40–7.30 (m, 18H, H-*b*,*c*), 7.25–7.20 (m, 12H, H-*a*), 6.87 (s, 6H, im *5′*), 5.07 (s, 12H, $-C^{\alpha}H_2$), 4.50 (m, 6H, His-$C^{\beta}H$), 3.05 (m, 6H, $-C^{\delta}H_2$), 2.89 (m, 6H, $-C^{\sigma}H_2$), 2.39 (m, 12H, His-$C^{\gamma}H_2$).

2.2.4. Synthesis of tris{[tris(benzyl-im-histidyl)aminoethyl}amine L^3

Hexa (0.76 g, 0.50 mmol) was added to an ice-cold solution of DCC (0.36 g, 1.72 mmol), HOBt (0.23 g, 1.50 mmol), and N(α)-(t-butoxycarbonyl-N(π)-benzyl-L-histidine (0.50 g, 1.50 mmol) in DMF (8 mL). The reaction mixture was worked up in a similar fashion as described for the synthesis of Boc-**Hexa**.

The protected BOC-$\mathbf{L^3}$: Yield: 0.74 g, 49%. $C_{138}H_{156}N_{31}O_{15}$ (2488.96): C, 66.59; H, 6.32; N, 17.45. Found: C, 65.04; H, 6.53; N, 17.93. ^{1}H NMR (400 MHz, $CDCl_3$, s = singlet, m = multiplet, br = broad): 7.41 (s, 9H, im *2′*), 7.30–7.24 (m, 27H, H-*b*,*c*), 7.22–7.18 (m, 18, aromatic, H-*a*), 6.79 (s, 9H, im *5′*), 5.91 (br, s, 9H, amide-NH), 5.24 (s, 18H, $-C^{\alpha}H_2$), 4.66 (m, 9H, His-$C^{\beta}H$), 3.39–3.28 (m, 6H, $-C^{\delta}H_2$), 3.12–3.07 (m, 18H, His-$C^{\gamma}H_2$), 2.88–2.81 (m, 6H, $^{-}C^{\sigma}H_2$), 1.42 (s, Boc, 81H).

The acidified $\mathbf{L^3}$-TFA: Yield: 0.77 g, 69%: Anal. Calc. for $C_{123}H_{132}N_{31}O_9\cdot 13CF_3COOH\cdot 5H_2O$ (2191.6 + 1482.3 + 90): C, 44.03; H, 3.92; N, 10.68. Found C, 44.65; H, 3.84; N, 10.57. ^{1}H NMR (400 MHz, D_2O, s = singlet, m = multiplet): 8.68 (s, 9H, im *2′*), 7.52–7.43 (m, 27H, H-*b*,*c*), 7.33–7.27 (m, 18H, H-*a*), 7.22 (s, 9H, im *5′*), 5.40 (s, 18H, $-C^{\alpha}H_2$), 4.61 (m, 9H, His-$C^{\gamma}H$), 4.41–4.37 (m, 6H, $-C^{\delta}H_2$), 3.48 (m, 6H, $-C^{\sigma}H_2$), 3.20–3.09 (m, 18H, His-$C^{\gamma}H_2$).

The ligand $\mathbf{L^3}$: Yield: 0.26 g, 57%: Anal. Calc. for $C_{123}H_{132}N_{31}O_9\cdot 4H_2O$ (3199.57 + 72.07): C, 65.26; H, 6.37; N 19.18. Found: C, 66.76; H, 6.01; N, 19.55. ^{1}H NMR (400 MHz, D_2O, s = singlet, m = multiplet): 7.64 (s, 9H, im *2′*), 7.39–7.33 (m, 27H, H-*b*,*c*), 7.29–7.22 (m, 18H, H-*a*), 6.84 (s, 9H, im *5′*), 5.12 (s, 18H, $-C^{\alpha}H_2$), 4.46 (m, 9H, His-$C^{\gamma}H$), 3.09 (m, 6H, $-C^{\delta}H_2$), 2.88 (m, 6H, $-C^{\sigma}H_2$), 2.37 (m, 18H, His-$C^{\gamma}H_2$).

2.2.5. Synthesis of the mononuclear zinc(II) complex (**2**)

The ligand $\mathbf{L^2}$ (50 mg, 0.04 mmol) was dissolved in 3 mL aqueous metanol (75%, *v*/*v*) and the pH was adjusted to 7.0 using 1.0 M HNO_3. Aqueous methanolic solution of $Zn(ClO_4)_2\cdot 6H_2O$ (30 mg, 0.08 mmol) was then added. A white precipitate was produced, filtered off by membrane filter, washed out by ether, and dried up in vacuo. Yield: 43 mg, 73%: Anal. Calcd. For $C_{48}H_{58}Cl_2N_{10}O_{19}Zn$ ($[\mathbf{L^2}Zn(OH_2)](ClO_4)_2\,H_2O$) (1197.31 + 18.02: C, 47.44; H, 4.81; N, 11.53; Cl, 5.83%. Found: C, 47.34; H, 4.92; N, 11.35; Cl, 5.79%. ^{1}H NMR (CD_3OD:D_2O, 3:1, *v*/*v*, s = singlet, m = multiplet): 7.83 (s, 2H; im *2′*), 7.49–7.42 (m, 6H; H-*b*,*c*), 7.33–7.25 (m, 4H; H-*a*), 7.07 (s, 4H; im *5′*), 5.22 (s, 4H; $-C^{\alpha}H_2$), 4.83–4.81 (m, 2H; His-$C^{\beta}H$), 3.66 (s, 6H; OCH_3), 3.56 (s, 4H; N-CH_2), and 3.18–3.10 ppm (m, 4H; His-$C^{\gamma}H_2$).

2.2.6. Synthesis of the trinuclear zinc(II) complex (**3**)

The ligand $\mathbf{L^3}$ (82 mg, 0.10 mmol) was dissolved in 2 ml MeOH: water (50%, *v*/*v*) and the pH was adjusted to 7.0 using 1.0 M HNO_3. Aqueous methanolic solution of $Zn(ClO_4)_2\cdot 6H_2O$ (37 mg, 0.10 mmol) was then added. A white precipitate was produced, filtered off by membrane filter, washed out by ether, and dried up in vacuo. Yield: 60 mg, 68%: Anal. Calc. for $C_{123}H_{154}N_{31}O_{53}Cl_9Zn_3$ ($[\mathbf{L^3}Zn_3(H_2O)_3](ClO_4)_6\cdot 3HClO_4\cdot 5H_2O$) (3039.52 + 301.38 + 90.08): C, 43.07; H, 4.53; Cl, 9.30; N, 12.65; Zn, 5.71%. Found: C, 42.45; H, 4.62; Cl, 9.25; N, 12.76; Zn, 5.76%. ^{1}H NMR (400 MHz, D_2O/DMSO-d_6 20:1, s = singlet, m = multiplet): 7.73 (s, 9H, im *2′*), 7.55–7.18 (m, 27H, H-*b*,*c*), 7.33–7.21 (m, 18H, H-*a*), 6.89 (s, 9H, im *5′*), 5.27–5.18 (s, 18H, $-C^{\alpha}H_2$), 4.64 (m, 9H, His-$C^{\beta}H$), 3.28–3.15 (m, 6H, $-C^{\delta}H_2$), 3.08–2.96 (m, 6H, $-C^{\sigma}H_2$), 2.54–2.43 (m, 18H, His-$C^{\gamma}H_2$).

2.3. Potentiometric measurements

Potentiometric titrations were carried out at 25.0 ± 0.2 °C with a TOA AUT-501 automatic titrator connected to a TOA ABT-511 automatic burette with a combined glass electrode. The electrode was calibrated using standard aqueous buffers. The ionic strength was adjusted to 0.1 M by adding appropriate amounts of $NaNO_3$. Solutions were made up with aqueous methanol (33%, *v*/*v*) and the ionic strength was adjusted to 0.1 M by adding appropriate amounts of $NaNO_3$. The glass electrode was calibrated and checked for linearity with standard borax and potassium hydrogen phthalate as well as acetate buffers. Checks for the presence of carbonate were made using a Gran plot and the determination of K_w for the solvent system. Although a correction was not made to compensate for the methanol–water liquid junction potential a correction of 0.136 pH units can be subtracted from the measured pH readings as suggested by Bates et al [65] to enable a comparison to be made with measurements in aqueous solution. All solutions were carefully protected from air by a stream of nitrogen. Solutions of 1.00 mM of $\mathbf{L^1}$ in the absence and in the presence of equivalent Zn^{2+} ion were titrated with 0.1 M NaOH aqueous solution. Equilibrium constants were calculated using the program BEST [66] and species distributions were calculated using the program SPE [66].

2.4. ^{1}H NMR measurements

To confirm stoichiometry of zinc complexes of each ligand, ^{1}H NMR analyses were undertaken in order to investigate the effect of pH and the added zinc on the shape and the chemical shift of ligand peaks. From the pH or R (=$[Zn^{2+}]_o/[\mathbf{L}]_o$)-dependence of chemical shifts, we can get more insight about that which protons are effected (thus shifted) most, i.e. gives evidence about the location of protonation/complexation sites [45,67]. The concentrations used were analogous to that was used in pH-titrations; ionic strength was kept constant at 0.1 M by using $NaNO_3$. D_2O was used as solvent for the titration of $\mathbf{L^1}$, while in case of $\mathbf{L^3}$, a solution of MeOH-d_4 and D_2O (33% *v*/*v*) was used. The concentration of the ligands (2×10^{-3} M) in D_2O and I = 0.1 M $NaNO_3$ was kept constant at a pH ≈ 7 at 30 °C. Chemical shifts are reported relative to the resonance signal of sodium 2,2-dimethyl-2-silapentane-5-sulfonate (DSS) as internal standard. The

pD was adjusted with concentrated NaOD and DNO_3, so that the effect of dilution could be neglected.

2.5. Hydrolysis reaction of the toxic organophosphate, parathion

The hydrolysis rate of parathion, DNTP catalyzed by Zn^{2+}-bound hydroxo species of (**1**), (**2**), and (**3**) in aqueous media was measured following an increase in 402 nm absorption of released *p*-nitrophenolate as a hydrolysis product [39–45]. Application of co-solvent was necessary in the case of $\mathbf{L^2}$ and $\mathbf{L^3}$ (MeOH:H_2O, 33%, *v*/*v*): reactions with $\mathbf{L^1}$ have been carried out in both H_2O and MeOH:H_2O (33%, *v*/*v*). The hydrolysis rate of parathion, DENTP (4.0×10^{-5} M) catalyzed by their zinc(II) complexes (**1**)–(**3**) (1.0×10^{-3} M) in aqueous methanol was measured following an increase in 402 nm absorption of released *p*-nitrophenolate as a hydrolysis product. The pH of each sample was adjusted by using 1 M $NaOH/HNO_3$, and not by using buffers in order to avoid any catalytic or inhibition effect. In the course of hydrolysis, the pH of each sample was checked and was found that the difference compared to the adjusted pH value at the beginning of hydrolysis was not larger than 0.3. The samples, included the organophosphate and both complexes were incubated at 30 °C, while the applied parathion concentration was 20 μM. All reactions showed first-order characteristics and were followed up to 5 half lives. Reaction rates are corrected by blank experiments which were made up similarly but without the presence of the zinc complexes. The pseudo-first order rate constants, as before, were estimated from the integrated form of the first-order law.

3. Results and discussion

3.1. Characterization of the ligands and their zinc(II) model complexes

The general aim of the synthesis of these artificial peptides is to mimic the structure of the *phosphohydrolase* active site by not only utilizing zinc as natural ion in zinc-containing enzymes, but also to incorporate peptides as the building blocks of large proteins. The increasing number of the attached histidyl units will come together with the formation of multinuclear zinc complexes. The benzylation of pyrrolic imidazole nitrogen in these ligands $\mathbf{L^1}$, $\mathbf{L^2}$, and $\mathbf{L^3}$ protects the imidazole ring of histidine from side reactions during synthesis and later will have an important role in zinc coordination since only the pyridine-type nitrogen of the imidazole ring will be available for coordination. The three histidyl residues coupled to nitrilotriacetic acid (NTA) in $\mathbf{L^2}$ and tris(2-aminoethyl)amine (TREN) in $\mathbf{L^1}$ and $\mathbf{L^3}$ *via* amide bond formations mimicked the histidine side chain in large proteins, which is common in the active site of several zinc enzymes.

We tried to attach benzyl groups to each histidyl unit in order to: (i) increase the hydrophobicity around zinc, (ii) avoid octahedral dimer formation by introducing benzyl groups as a steric hindrance, and (iii) help binding of aromatic substrates by π–π stacking. The advantageous of these ligands can be summarized in the following statements: (i) the donation sites of imidazoles have kinetically more labile binding ability, (ii) there is a larger spacer distance between the imidazole donor set and the tertiary nitrogen, (iii) there is an increased flexibility for coordination thus forming a more optimal geometry, and (iv) for steric reasons, it is impossible to bind the central tertiary nitrogen.

3.1.1. Deprotonation and zinc complexation constants of L^1 and L^2

The obtained ligands: $\mathbf{L^1}$, $\mathbf{L^2}$, and $\mathbf{L^3}$ provided an opportunity to examine the effect of changing the number of histidine side chains on the ligand deprotonation and complexation constants, and nevertheless on the pK_a of the coordinated water molecule. Typical set of species distribution curves for $\mathbf{L^1}$ and $\mathbf{L^2}$ in the presence of stoichiometric amounts of Zn^{2+} are shown in Figs. 1 and 2. While in case of ligand $\mathbf{L^3}$, the number of ligation sites far exceeds the capacity of the fitting program, so no attempts were made to measure and to evaluate the pH-metric curves. The obtained deprotonation constants pK_a are summarized in Table 1. In ligand $\mathbf{L^2}$, three consecutive deprotonation steps were observed and assigned to the three imidazole nitrogens (Table 1). In dipeptides, where the amino group of histidine is unprotected, the pK_a of the imidazole nitrogens is lower than in histidine: e.g. 5.39 in His-Gly, 5.65 in His-Leu while this value is 5.87 in histidine [68,69]. Thus, $\mathbf{L^2}$ has more basic imidazole nitrogens [70,71] because it lacks other aliphatic nitrogens, which is found in $\mathbf{L^1}$ [60,72–74], where the presence of these aliphatic amines makes the imidazol groups more acidic.

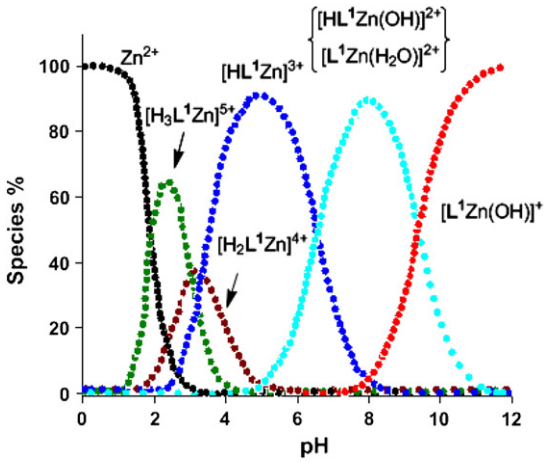

Fig. 1. Distribution curve of zinc-containing species of 1.0×10^{-3} M of $\mathbf{L^1}$ in the presence of equivalent amount of Zn^{2+} ions in aqueous methanol (33%, *v*/*v*) at $I=0.1$ M $NaNO_3$ and 30 °C.

The potentiometric pH titration curve for the ligands $\mathbf{L^1}$ and $\mathbf{L^2}$ in the presence of equimolar Zn^{2+} revealed complex formations until [OH]/[**L**] = 7.0 [61] and 3.0, respectively. But in all cases Zn complexes reacted with more OH^- than what was needed to fully deprotonate the ligands. This means each complex contains one extra deprotonable group which is not present in the ligands themselves. In the case of complex (**2**), the extra deprotonation can only be assigned to the deprotonation of water molecule ligated to the central zinc ion of the complex. In the case of complex **1**, the extra deprotonation could be assigned to two different processes: (i) deprotonation of the coordinated water molecule or (ii) metal-promoted deprotonation of the amide. Rabenstein et al. [67] showed that zinc(II)-promoted deprotonation of amide nitrogens in imidazole-containing peptides generally results in kinetically stable complexes. The chemical shifts of the protons near to the amide nitrogen are considerably altered. In

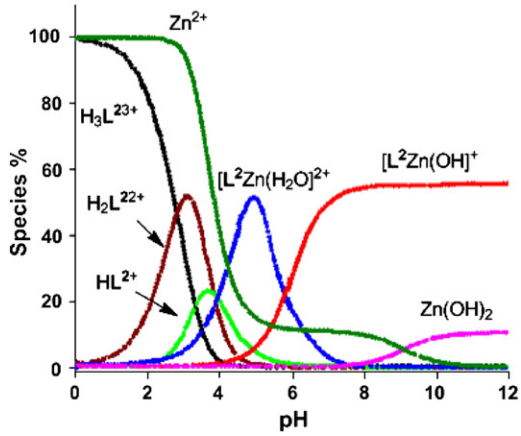

Fig. 2. Distribution curve of zinc-containing species of 1.0×10^{-3} M of $\mathbf{L^2}$ in the presence of equivalent amount of Zn^{2+} ions in aqueous methanol (33%, *v*/*v*) at $I=0.1$ M $NaNO_3$ and 30 °C.

Table 1
Stability constants ($\log K_{st}$) and deprotonation constants ($pK_a(H_2O)$ of $\mathbf{L^2}$ and its zinc(II) complex species.

Species/reactions	pK_a	$\log K_{st}$	pK_a (H_2O)
$HL^+ = L + H^+$	5.78		
$H_2L^+ = HL^+ + H^+$	5.23		
$H_3L^{3+} = H_2L^{2+} + H^+$	4.36		
$L + Zn^{2+} = LZnOH_2^+$		3.95	
$LZnOH_2^+ = LZnOH^+ + H^+$			7.33

order to clarify whether the amide nitrogens are coordinated to zinc or not, we have conducted ^{1}H NMR titration measurements for ligand $\mathbf{L^1}$ (2.0×10^{-3} M) in the presence of equimolar amount of Zn^{2+} ion in D_2O (Fig. 3) as a function of pD (above pD 6.0). Through this, we found out that the methylene protons of the TREN part (β), directly linked to the amide nitrogens were weakly influenced (0.03 ppm). The above result strongly indicates that the extra deprotonation is only related to the formation of zinc-bound hydroxo species and not with metal-promoted deprotonation of amide nitrogens.

The obtained stability constants $\log K_{st}$ and deprotonation constants $pK_a(H_2O)$ of zinc complexes (**1**) and (**2**) are listed in Table 2. The potentiometric data indicated that $\mathbf{L^2}$ forms a less stable complex with Zn(II) ($\log K_{st} = 3.95$). The lowering in $\log K_{st}$ value of (**2**) is consistent with related complexes bearing only 3 imidazole donor functions [70,71] and is consistent with the protonated species $[H_3\mathbf{L^1}Zn]^{5+}$ of the ligand $\mathbf{L^1}$. The lowering $pK_a(H_2O)$ in both complexes: (**1**) (7.43), and (**2**) (7.33) may arise because of the bulkiness around each coordinated water molecule. *N*-alkylation of the pyrrolic nitrogen in imidazole units reduces the metal binding ability of the ligand. For example in the case of tripodal *N*-methyl imidazole derivatives, $\log K_{st}$ decreases about 3–4 units, with a $\log K_{st}$ value of around 4, which is consistent with the analogous value of $[H_3\mathbf{L^1}Zn]^{5+}$ species [70,71]. Subsequent deprotonation of aliphatic amino groups forms complexes with increasing $\log k_{st}$ values indicating some contribution of amino nitrogens in coordination with the central zinc ion.

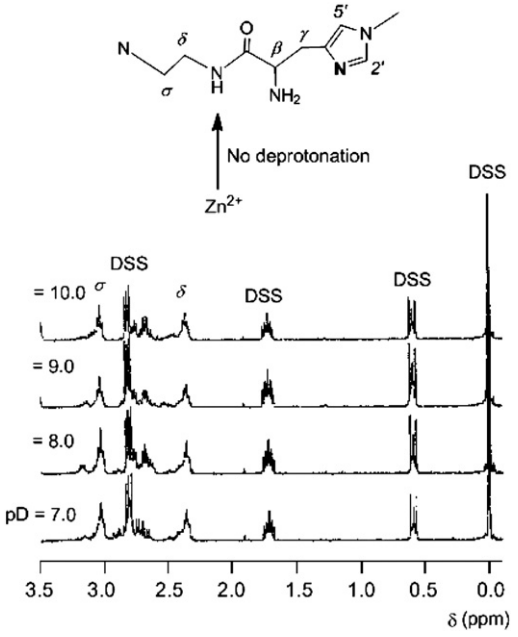

Fig. 3. Upfield region for the methylene protons of the TREN part (a and b) linked to the amide nitrogens for $\mathbf{L^1}$ (2.0×10^{-3} M) in the presence of equimolar amount of Zn(II) (2.0×10^{-3} M) as a function of pD in deutrated aqueous methanol: D_2O:CD_3OD (33%, *v*/*v*) at $I = 0.1$ M $NaNO_3$ and 30 °C.

Table 2
Stability constant ($\log K_{st}$) and deprotonation constant ($pK_a(H_2O)$ of the indicated species of zinc(II) complex **2.**

Species/reaction	$\log K_{st}$	pK_a (H_2O)
$\mathbf{L^2} + Zn^{2+} = \mathbf{L^2}Zn^{2+}$	3.95	3.95
$\mathbf{L^2}ZnOH_2^{2} = \mathbf{L^2}ZnOH^{2+} + H^+$		7.33

The monoprotonated complex species, $[H\mathbf{L^1}Zn(H_2O)]^{3+}$ contains zinc-bound water molecule and one protonated primary amino group. The proton loss of this species can occur either at the amino function to form $[\mathbf{L^1}Zn(H_2O)]^{2+}$ ($pK_a = 8.38$) or at the coordinated water molecule to form $[H\mathbf{L^1}Zn(OH)]^{2+}$ ($pK_a = 7.43$). As these species are titrimetrically equivalent, it is not possible to distinguish between them by pH-metric titration. Since the stability of $[H\mathbf{L^1}Zn(OH)]^{2+}$/$[\mathbf{L^1}Zn(H_2O)]^{2+}$ is not much higher compared to $[H\mathbf{L^1}Zn(H_2O)]^{3+}$, it indicates that $[H\mathbf{L^1}Zn(OH)]^{2+}$/$[\mathbf{L^1}Zn(H_2O)]^{2+}$ contains no new coordination site in comparison with $[H\mathbf{L^1}Zn(H_2O)]^{3+}$. A possible newly formed binding site would probably contribute to ligate the central zinc, resulting in higher $\log k_{st}$ values. If the $[H\mathbf{L^1}Zn(H_2O)]^{2+}$ is formed, there is no increase in the coordination number of the central zinc and is not associated with dramatic change in $\log K_{st}$. From the above reasons we assume that when $[H\mathbf{L^1}Zn(H_2O)]^{3+}$ loses a single proton, the zinc-bound hydroxo species, rather than the $[\mathbf{L^1}Zn(H_2O)]^{2+}$ is formed.

3.1.2. pD and R (=$[Zn^{2+}]_o/[L]_o$)-dependent ^{1}H NMR titrations

To get additional information about the pD-dependence of complex formation between zinc and the different ligands, another set of experiments has been performed where the zinc-to-ligand ratio was kept constant and the pD of the solution was varied. The aromatic region of the spectra is shown in separate charts in Fig. 4. The free ligand $\mathbf{L^1}$ (R = 0.0) demonstrates strong upfield shift between pD 4.0 and 6.0, especially the 2′-imidazole peak is influenced and is in relation with the proton loss of the pyridine-type of the imidazole nitrogens. When pD is increased, slight upfield shift for the imidazole peaks are observed which is due to the deprotonation of the primary amino nitrogen.

At R = 1.0 there is no change found at pD 4, in comparison with the free form at the same pD indicating that even in presence of 1.0 equivalent of zinc, no complexation takes place at this pD. At pD 5.0, broadening of imidazole peaks indicates at least partial formation of the mononuclear $[H_3\mathbf{L^1}Zn]^{5+}$ complex. At pD higher than 7.0, the imidazole peaks show change in chemical shift and peak shape when compared to the spectrum of the free ligand. The deprotonation process of $[H\mathbf{L^1}Zn(H_2O)]^{3+} \leftrightarrow \{[H\mathbf{L^1}Zn(OH)]^{2+} + [\mathbf{L^1}Zn(H_2O)]^{2+}\} + H^+$ was described by a pK_a of 7.43 by pH-titration, but since mixture of aqua and hydroxo species are yielded, the effect of hydroxo species formation is hardly seen in the pD-dependent ^{1}H NMR spectra. At pD 9.0, broadening of all aromatic peaks is observed, and can be related to the appearance of $[\mathbf{L^1}Zn(OH)]^+$ species, which is present in around 20% according to the distribution curve calculated from the pH-metric titration.

^{1}H NMR spectra for the R-dependence of $\mathbf{L^3}$ is presented in Fig. 5. The $\mathbf{L^3}$ contains tripeptide units in the side chains, the number and the ratios of different types of binding sites in this ligand makes it a special representative of artificial histidine-containing peptides. As shown in Fig. 5, in case of free ligand $\mathbf{L^3}$ ligand, all peaks are well resolved. When increasing R from 0.0 to 1.0, significant changes in both peak positions and peak shapes were recorded. At R = 0.5, the singlet peaks of 2′ and 5′-imidazolyl protons as well as phenyl protons show broadening and shifts downfield, which is clear indication about the fast chemical exchange between the complexed and uncomplexed $\mathbf{L^3}$. At R = 1.0 the aromatic peaks show some shift. This indicates that in mononuclear complexes only third of the 9 histidines take part in binding to zinc. When R is increased from 1.0 to 3.0, all peaks show considerable

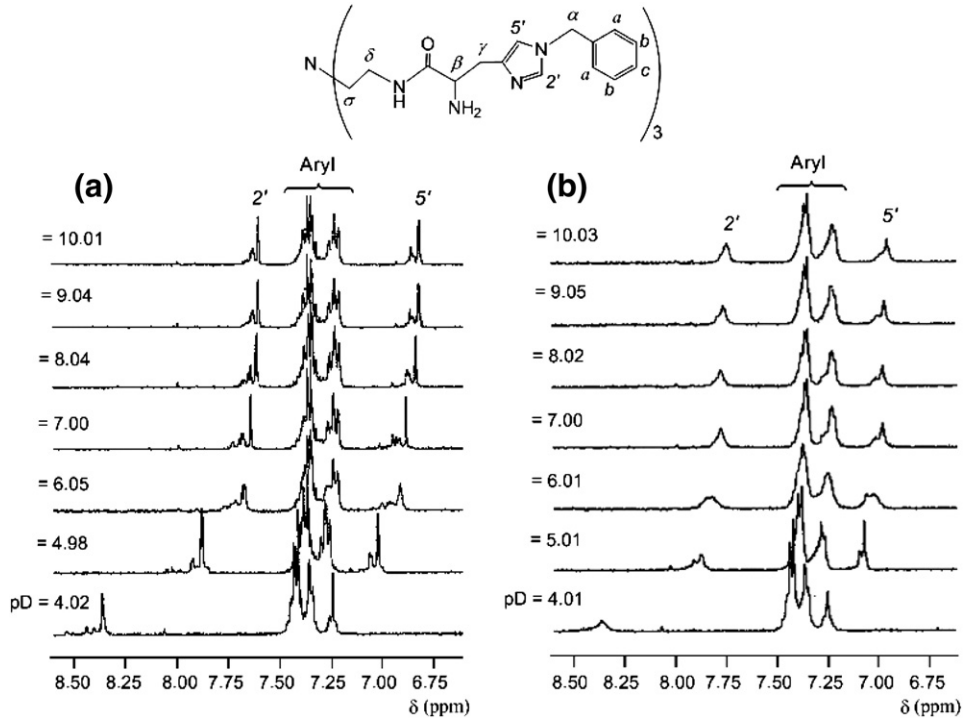

Fig. 4. Downfield region for the imidazole (2′ and 5′) and phenyl protons of the free ligand $\mathbf{L^1}$ (left) and in the presence of equimolar amount of zinc(II) (2.0×10^{-3} M) (right) as a function of pD in deutrated aqueous methanol: D_2O:CD_3OD (33%, *v*/*v*) at $I = 0.1$ M $NaNO_3$ and 30 °C.

broadening and shifting downfield, and when further zinc is added, no change is observed in peak shapes and positions. This clearly proves that the maximum stoichiometry of zinc-$\mathbf{L^3}$ complex is 3:1.

3.2. Hydrolysis of parathion by using zinc(II) model complexes (*1*) and (*3*)

The histidine units attached to the different oligoamine cores through peptide bond model the histidine side chains of the active site of *phosphohydrolase* enzymes [3–5]. The purpose of using zinc as a complexing ion was to keep the structural similarity between the native system and our model compounds. In order to show that these zinc complexes do not only serve as structural mimics, kinetic studies

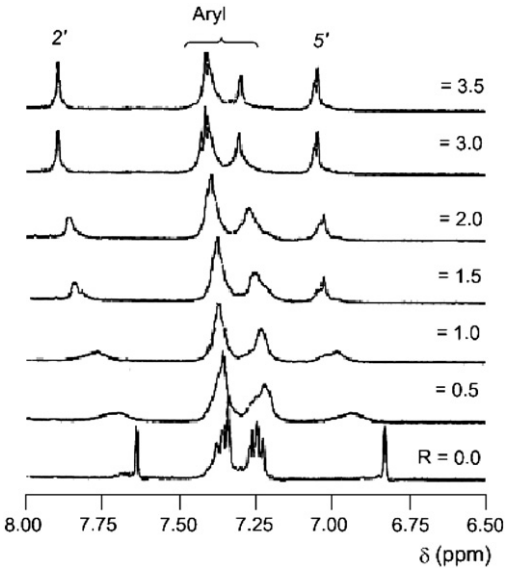

Fig. 5. Downfield region for the imidazole (2′ and 5′) and phenyl protons of the free ligand $\mathbf{L^3}$ (2.0×10^{-3} M) as a function of $R = [Zn^{2+}]_o/[\mathbf{L^3}]_o$ at pD 8.5 in deutrated aqueous methanol: D_2O:CD_3OD (33%, *v*/*v*) at $I = 0.1$ M $NaNO_3$ and 30 °C.

have been carried out to investigate the effect of the presence of histidine-containing peptide–zinc complexes on the hydrolysis rate of the toxic organophosphate, parathion (DENTP). In this part we report the results of a series of experiments carried out at different pH and zinc-to-ligand ratios. From these profiles we make suggestion about the active species, and from the comparison of activities of different complexes we attempt to propose reaction mechanism and some comments on the structure of zinc complexes are also made.

The catalytic activity of zinc(II) complex (**1**) with maximum stoichiometry is strongly influenced by the pH of the reaction mixture. The cleavage of parathion was followed by monitoring the increase in the visible absorbance at 400 nm caused by release of the *p*-nitrophenolate ion. The values of pseudo-first-order rate constants, k_{obs} (Table 2) obtained from the semilogarithmic plots for the hydrolysis of reaction at different pH values in aqueous methanol (33%, *v*/*v*) (Supplementary material, S1) were linear, confirming the first order dependence on the substrate concentration. The pH-dependence of the pseudo-first order rate constants on the hydrolysis of parathion promoted by the zinc complex (**1**) with the maximum stoichiometry (Fig. 6) displayed bell-shaped curve with the maximum rate constant of 1.36×10^{-5} s^{-1} at pH 8.5. Bell-shaped profiles (fitted by Lorentzian function, 4 parameters) are seen in a number of phosphate ester hydrolysis promoted by zinc complexes, and are indicative of the involvement of the nucleophilic zinc-hydroxo [60,61,74]. This rate profile largely correlates with the distribution curve of species {$[H\mathbf{L^1}Zn(OH)]^{2+}$/$[\mathbf{L^1}Zn(H_2O)]^{2+}$}. Below and above pH 8.5 the rate constants decrease with the simultaneous decrease of the percentage of the above mentioned species. The results of pH-metric titration suggested the coexistence of two species with maximum abundance at pH 8.5: one is with zinc-bound water, $[\mathbf{L^1}Zn(H_2O)]^{2+}$ while another is zinc-bound hydroxo species, $[H\mathbf{L^1}Zn(OH)]^{2+}$. In latter species, one of the terminal amino group is protonated. It was not possible to distinguish between these two species by means of pH-metric titration due to their tautomeric structure. If the aquated species played role in the hydrolysis, the zinc-bound water would not be sufficiently strong as general base, compared to the hydroxo-species. At pH below 7.0, where only water bound species exist as major species, a significantly diminished activity

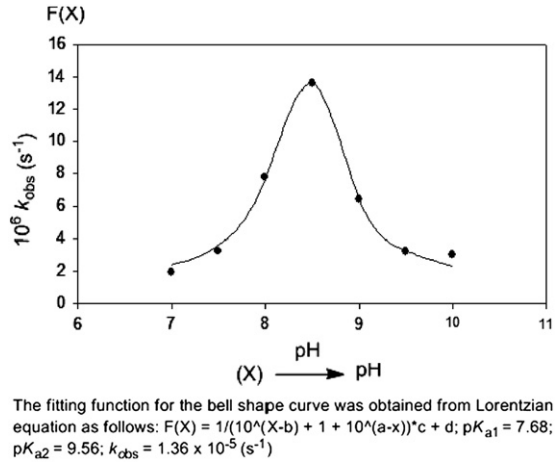

Fig. 6. Plots of the hydrolysis rate constant, k_{obs} of 4.0×10^{-5} M parathion (DENTP) by using zinc(II) complex (**1**) (1.0×10^{-3} M) at different pH values (● observed values and fitted curve by Lorentzian function, 4 parameters) in aqueous methanol (33%, *v*/*v*) at $I = 0.1$ M $NaNO_3$ and 30 °C.

of $[\mathbf{L^1}Zn(H_2O)]^{2+}$ is found which means that aqua-species solely cannot be active catalysts for DENTP hydrolysis. In parallel with this, at pH higher than 9.0, the percentage of aquated species is decreasing with the concomitant decrease of the rate constants, which is clear indication about that merely hydroxo-complex species possess lower activity than in the presence of aquated $[\mathbf{L^1}Zn(H_2O)]^{2+}$. It is interesting to observe that in the pH range 9.0−10.0, the rate constants do not fall that drastically as the percentage of $\{[H\mathbf{L^1}Zn(OH)]^{2+}/[\mathbf{L^1}Zn(H_2O)]^{2+}\}$ species. This may suggest that $[\mathbf{L^1}Zn(H_2O)]^{2+}\}$ also possesses some activity, but with considerably lower value compared to what is found in the case of $[H\mathbf{L^1}Zn(OH)]^{2+}/[\mathbf{L^1}Zn(H_2O)]^{2+}$. The mechanism for the hydroxo-complex catalyzed reaction probably follows an analogous pathway as was discussed for $[\mathbf{L^1}Zn(OH)]^{+}$ (see above). The higher activity of $[H\mathbf{L^1}Zn(H_2O)]^{2+}$ can be related to the decreased pK_a value of the coordinated water molecule: the proton loss in the process of $[H\mathbf{L^1}Zn(H_2O)]^{3+} \leftrightarrow \{[H\mathbf{L^1}Zn(OH)]^{2+} + H^+$ has a pK_a of 7.68, which is significantly lower than the pK_a for $[\mathbf{L^1}Zn(H_2O)]^{2+} \leftrightarrow [\mathbf{L^1}Zn(OH)]^{+} + H^+$ which was determined to be 8.70, thus the nucleophilicity of the bound-hydroxide can be higher in $\{[H\mathbf{L^1}Zn(OH)]^{2+}$ than in $[\mathbf{L^1}Zn(OH)]^{+}$. From the pK_a values of $\mathbf{L^1}$, $H\mathbf{L^1}^{+}$ species exists around pH 7.9 and above pH 8.0 this species gradually decreases, i.e., the $[H\mathbf{L^1}Zn(OH)]^{2+}$ also decreases. Around pH 10.5 $[\mathbf{L^1}Zn(OH)]^{+}$ exists in solution, while zinc-bound water complex is absent. A question then arises as to why $[\mathbf{L^1}Zn(OH)]^{+}$ is practically inactive in this process. A probable explanation can come from the coordination properties of this species. Since the proton loss step of $[HL^1Zn(OH)]^{2+}$ occurs in one of the primary amino function, the fully deprotonated complex contains one more ligation site, which may also coordinate to zinc. A possible increase in coordination number of zinc may radically change the conformation of the complex thus making it difficult for OH^- to interact with the substrate. The hydrophobic benzyl groups attached to the imidazole binding sites can serve as hydrophobic microenvironment but due to their bulkiness, can also sterically hinder the approach of the substrate. In the catalytic mechanism for the action of the species $[H\mathbf{L^1}Zn(OH)]^{2+}/[\mathbf{L^1}Zn(H_2O)]^{2+}$ (Scheme 5), they play a cooperative role for the hydrolysis of parathion through the Lewis acid mechanism. The zinc bound-OH species, acts as a nucleophile for acceleration of the hydrolysis reaction, while water-coordinated Zn species can supply proton as general Lewis acid holding the substrate for OH^- attack. The bound-hydroxide in $[H\mathbf{L^1}Zn(OH)]^{2+}$ can attack the phosporus, and through a pentacoordinated transition state, the leaving group *p*-nitrophenolate is released. The formed diethyl thiophosphate bound to the catalyst can be replaced by another molecule of DENTP and the catalytic cycle can be started again. The R ($=[Zn^{2+}]_o/[\mathbf{L}]_o$)-dependence study was carried out in ligand $\mathbf{L^3}$ to demonstrate the effect of the degree of complexation on the catalytic activity on the hydrolysis reaction. The applied range of R for the ligands was decided on the basis of the R-dependent ^1H NMR titration results. The values of pseudo-first-order rate constants, k_{obs} (Table 3) obtained from the semilogarithmic plot for the hydrolysis of parathion at different $Zn^{2+}/\mathbf{L^3}$ ratios in aqueous methanol (33%, *v*/*v*) at pH 8.5 (Supplementary materials, S2) were linear, confirming the first order dependence on the substrate concentration. The plot of the rate constants as a function of zinc-to-ligand ratio (R) is shown in Fig. 7.

Ligand $\mathbf{L^3}$ can form a trinuclear zinc complex which is the possible maximum stoichiometry as it was demonstrated from ^1H NMR titrations. The R-dependence of rate constants for $\mathbf{L^3}$ showed extremely low activity below R = 1, even lower than the complexes of $\mathbf{L^1}$. This can be explained by the higher coordination number of zinc, more precisely the larger variety of donor groups in $\mathbf{L^3}$ in comparison with the $\mathbf{L^1}$ (Table 4). The highly coordinated central zinc in the mononuclear complex of $\mathbf{L^3}$ might reduce the nucleophilicity of the bound-water molecule, and at the same time, may leave no sufficient free space around the coordinated water to interact with the phosphoester substrate. The rate constants increase sharply between

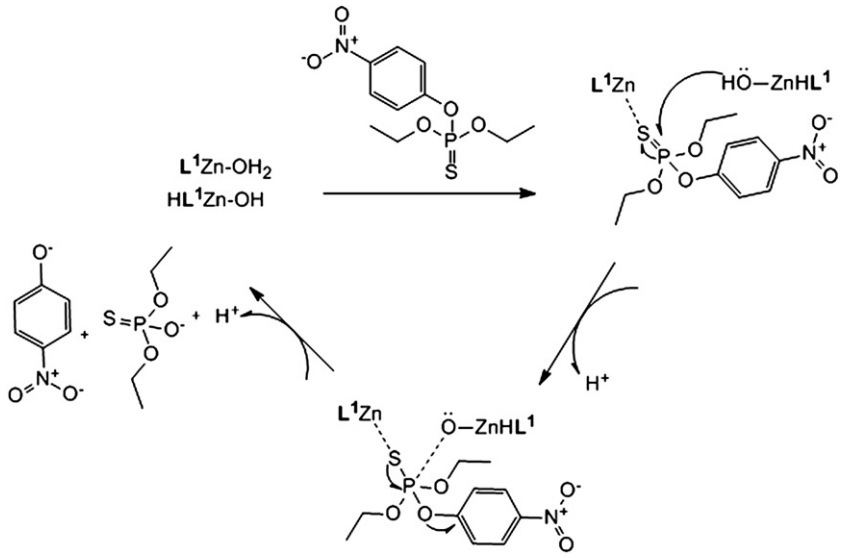

Scheme 5. The proposed mechanism for the hydrolysis of parathion by using zinc(II) complex (**1**).

Table 3
The observed pseudo-first order rate constants (k_{obs} (s^{-1})) for the cleavage of parathion (DNTP) (4.0×10^{-5} M) by using zinc(II) complex (**1**) (1.0×10^{-3} M) at different pH values in aqueous methanol (33%, *v*/*v*) at $I=0.1$ M $NaNO_3$ and 30 °C.

pH	10^6 k_{obs} (s^{-1})
7.0	1.96
7.5	3.26
8.0	7.77
8.5	13.60
9.0	6.44
9.5	3.24
10.0	3.03

Table 4
The observed pseudo-first order rate constants (k_{obs} (s^{-1})) for the cleavage of parathion (DNTP) (4.0×10^{-5} M) as a function of $R=[Zn^{2+}]_o/[\mathbf{L^3}]_o$ at pH 8.5 in aqueous methanol (33%, *v*/*v*) at $I=0.1$ M $NaNO_3$ and 30 °C.

$R=[Zn^{2+}]_o/[\mathbf{L^3}]_o$	10^5 k_{obs} (s^{-1})
0.5	0.704
1.0	1.52
1.5	1.69
2.0	3.08
2.5	4.20
3.0	4.54
3.5	4.47

1/1 and 3/1 zinc-to-ligand ratio which indicates the high catalytic activity of the formed trinuclear complex of $\mathbf{L^3}$. Since the rate acceleration is 3-fold for $\mathbf{L^3}$ when considering the rate constants of $R=3$ in comparison with $R=1$, cooperation between the catalytic zinc centers is indicated. The rate constants level off above $R=3$, which is in consistence with the ^{1}H NMR-titration results that showed 3/1 as maximum complex stoichiometry. When ligand $\mathbf{L^3}$ in itself was applied, moderate cleavage rates have been observed, smaller than the values for the reactions catalyzed by zinc(II) complex (**3**). Because of the lack of cooperation between zinc(II) ions in (**1**), the catalytic activity of (**3**) can be thought as resulting from the sum of contributions from three mononuclear arrangements as previously discussed in connection with the reactivity of other trinuclear zinc(II) complexes of calix[4]arene based ligands [12–16]. However, the trizinc complex (**3**) is only *ca* 3–4 fold more reactive than the mononuclear reference (**1**), indicating that cooperative action of the three zinc centers is limited. This could be attributed to the non-bridging spaceres between the three trihistidyl units (i.e., the lack or the weak coordination of zinc ions with the tertiary nitrogen atoms of the TREN part) produces very little pre-organization of the structure [75]. Due to the complexity of this system, it is difficult to obtain exact analysis on this dynamic complexation system.

4. Conclusion

Based on the mononucleating ligand $\mathbf{L^1}$, two new histidine-containing artificial tri- and nonapeptides $\mathbf{L^2}$ and $\mathbf{L^3}$ were prepared. Zinc(II) binding studies by these ligand systems were analyzed by means of potentiometric and ^{1}H NMR titrations in aqueous methanol (33% *v*/*v*). Subsequently their zinc(II) complexes (**1**), (**2**), and (**3**), respectively were synthesized and fully characterized. The activity of these zinc complexes are tested on the hydrolysis of the toxic organophosphate, parathion (DENTP). Complexes (**1**) and (**3**) are indeed highly reactive, producing in the case of (**3**) an ~25,000-fold rate acceleration over the background reaction at pH 8.5 and 30 °C. However, the trizinc complex (**3**) is only ~3 fold more reactive than the mononuclear reference (**1**), indicating that cooperative action of the three zinc centers is limited. This could be attributed to the non-bridging spacers between the three trihistidyl moieties (i.e., the lack or the weak coordination of zinc ions with the tertiary nitrogen atoms of the TREN part) produces very little pre-organization of the structure. The results obtained, in turn, were able to provide certain clues to the nature of the mechanism of action of this new trizinc nonahistidine complex (**3**). But due to the complexity of this system, it is difficult to obtain exact analysis on this dynamic complexation system.

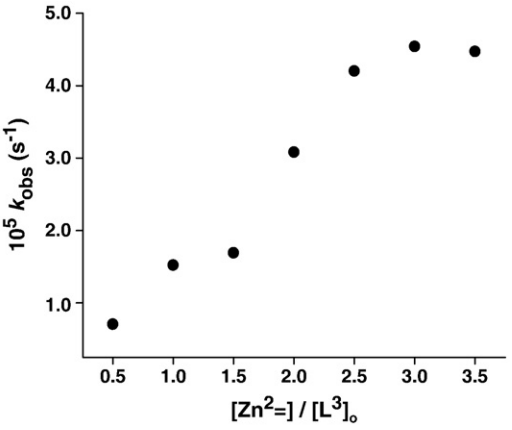

Fig. 7. Plots of the hydrolysis rate constant, k_{obs} of 4.0×10^{-5} M parathion (DENTP) as a function of $R=[Zn^{2+}]_o/[\mathbf{L^3}]_o$ at pH 8.5 in aqueous methanol (33%, *v*/*v*) at $I=0.1$ M $NaNO_3$ and 30 °C.

Appendix A. Supplementary data

Supplementary data associated with this article can be found, in the online version, at doi:10.1016/j.jinorgbio.2010.07.009.

References

[1] Y.-C. Yang, J.A. Baker, J.R. Ward, Chem. Rev. 92 (1992) 1729.
[2] Y.-C. Yang, Acc. Chem. Res. 32 (1999) 109.
[3] M.J. Jedrzejas, P. Setlow, Chem. Rev. 101 (2001) 607.
[4] D.E. Wilcox, Chem. Rev. 96 (1996) 2435.
[5] N. Sträter, W.N. Lipscomb, T. Kablunde, B. Krebs, Angew. Chem. Int. Ed Engl. 35 (1996) 2025.
[6] J.R. Morrow, O. Iranzo, Curr. Opin. Chem. Biol. 8 (2004) 192.
[7] P. Molenveld, J.F.J. Engbersen, D.N. Reinhoudt, Chem. Soc. Rev. 29 (2000) 75.
[8] E. Kimura, Curr. Opin. Chem. Biol. 4 (2000) 207.
[9] H. Williams, B. Takasaki, M. Wall, J. Chin, Acc. Chem. Res. 32 (1999) 485.
[10] E.L. Hegg, J.N. Burstyn, Coordin. Chem. Rev. 173 (1998) 133.
[11] A. O'Donoghue, S.Y. Pyun, M.-Y. Yang, J.R. Morrow, J.P. Richard, J. Am. Chem. Soc. 128 (2006) 1615.
[12] R. Cacciapaglia, A. Casnati, L. Mandolini, D.N. Reinhoudt, R. Salvio, A. Sartori, R. Ungaro, Inorg. Chim. Acta 360 (2007) 981.
[13] R. Cacciapaglia, A. Casnati, L. Mandolini, D.N. Reinhoudt, R. Salvio, A. Sartori, R. Ungaro, J. Org. Chem. 70 (2005) 624.
[14] R. Cacciapaglia, A. Casnati, L. Mandolini, D.N. Reinhoudt, R. Salvio, A. Sartori, R. Ungaro, J. Org. Chem. 70 (2005) 5398.
[15] R. Cacciapaglia, A. Casnati, S. Di Stefano, L. Mandolini, D. Paolemili, A. Sartori, D.N. Reinhoudt, R. Ungaro, Chem. Eur. J. 10 (2004) 4436.
[16] R. Cacciapaglia, S. Di Stefano, L. Mandolini, J. Am. Chem. Soc. 125 (2003) 2224.
[17] F. Mancin, E. Rampazzo, P. Tecilla, U. Tonellato, Eur. J. Org. Chem. (2004) 281.
[18] C. Bazzicalupi, A. Bencini, E. Berni, A. Bianchi, P. Fornasari, C. Giorgi, B. Valtancoli, Inorg. Chem. 43 (2004) 6255.
[19] S. Takebayashi, M. Ikeda, M. Takeuchi, S. Shinkai, Chem. Commun. (2004) 420.
[20] N.C. Gianneschi, S.-H. Cho, S.T. Nguyen, C.A. Mirkin, Angew. Chem. Int. Ed. 43 (2004) 5503.
[21] O. Iranzo, J.P. Richard, J.R. Morrow, Inorg. Chem. 43 (2004) 1743.
[22] K. Worm, F. Chu, K. Matsumoto, M.D. Best, V. Lynch, E.V. Anslyn, Chem. Eur. J. 9 (2003) 741.
[23] I.O. Fritsky, R. Ott, H. Pritzkow, R. Krämer, Chem. Eur. J. 7 (2001) 1221.
[24] J. Chin, Curr. Opin. Chem. Biol. 1 (1997) 514.
[25] T. Tanase, J.W. Yun, S.J. Lippard, Inorg. Chem. 35 (1996) 3585.
[26] H. Kurosaki, T. Tawada, S. Kawasoe, Y. Ohashi, M. Goto, Bioorg. Med. Chem. Lett. 10 (2000) 1333.
[27] T. Gajdá, R. Krämer, A. Jancsó, Eur. J. Inorg. Chem. (2000) 1635.
[28] P.E. Jurek, A.E. Martell, Inorg. Chem. 38 (1999) 6003.
[29] J. Du Bois, T.J. Mizoguchi, S.J. Lippard, Coord. Chem. Rev. 200 (2000) 443.
[30] B. Bosnich, Inorg. Chem. 38 (1999) 2554.
[31] R.D. Adams, F.A. Cotton (Eds.), Catalysis by Di- and Polynuclear Metal Cluster Complexes, Wiley-VCH, New York, 1998.

[32] G.J. Rowlands, Tetrahedron 57 (2001) 1865.
[33] R. Mathews, C.S. Rossiter, J.R. Morrow, J.P. Richard, Dalton Trans. (2007) 3804.
[34] L. Bonfa, M. Gatos, F. Mancin, P. Tecilla, U. Tonellato, Inorg. Chem. 42 (2003) 3943.
[35] T. Itoh, H. Hisada, Y. Usui, Y. Fujii, Inorg. Chim. Acta 283 (1998) 51.
[36] Y. Fujii, T. Itoh, K. Onodera, T. Tada, Chem. Lett. (1995) 305.
[37] J. Morrow, Comments Inorg. Chem. 29 (2008) 169.
[38] G. Feng, J.C. Mareque-Rivas, R.T.M. De Rosales, N.H. Williams, J. Am. Chem. Soc. 127 (2005) 13470.
[39] M.M. Ibrahim, K. Ichikawa, M. Shiro, Inorg. Chim. Acta 353 (2003) 187.
[40] T. Echizen, M.M. Ibrahim, K. Nakata, M. Izumi, K. Ichikawa, M. Shiro, J. Inorg. Biochem. 98 (2004) 1347.
[41] M.M. Ibrahim, Inorg. Chem. Commun. 9 (2006) 1215.
[42] M.M. Ibrahim, G.M. Mersal, J. Inorg. Organomet. Polym. 19 (2009) 549.
[43] M.M. Ibrahim, K. Ichikawa, M. Shiro, Inorg. Chem. Commun. 6 (2003) 1030.
[44] M.M. Ibrahim, S.Y. Shaban, K. Ichikawa, Tetrahedron Lett. 49 (2008) 7303.
[45] M.M. Ibrahim, J. Inorg. Organomet. Polym. 19 (2009) 532.
[46] H. Linjalahti, G. Feng, J.C. Mareque-Rivas, S. Mikkola, N.H. Williams, J. Am. Chem. Soc. 130 (2008) 4232.
[47] G. Feng, D. Natale, R. Prabaharan, J.C. Mareque-Rivas, N.H. Williams, Angewandte Chemie Int. Ed. Engl. 45 (2006) 7056.
[48] G. Feng, J.C. Mareque-Rivas, N.H. Williams, Chem. Comm. 1845 (2006).
[49] R. Cacciapaglia, A. Casnati, L. Mandolini, D.N. Reinhoudt, R. Salvio, A. Sartori, R. Ungaro, J. Am. Chem. Soc. 128 (2006) 12322.
[50] C. Bazzicalupi, A. Bencini, E. Berni, C. Giorgi, S. Maoggi, B. Valtancoli, Dalton Trans. (2003) 3574.
[51] S.R. Korupoju, N. Mangayarkarasi, P.S. Zacharias, J. Mizuthani, H. Nishihara, Inorg. Chem. 41 (2002) 4099.
[52] T. Nittymäki, H. Lönnberg, Org. Biomol. Chem. 4 (2006) 15.
[53] U. Kaukinen, L. Bielecki, S. Mikkola, R.W. Adamiak, H. Lönnberg, J. Chem. Soc. Perkin Trans. 2 (2001) 1024.
[54] T. Koike, E. Kimura, J. Am. Chem. Soc. 113 (1991) 8935.
[55] M. Yashiro, A. Ishikubo, M. Komiyama, J. Chem. Soc. Chem. Commun. (1997) 83 (a).
[56] S. Matsuda, M. Yashiro, A. Kuzuka, A. Ishikubo, M. Komiyama, Angew. Chem. Int. Ed. 37 (1998) 3284.
[57] M. Komiyama, S. Kina, K. Matsumura, J. Sumaoka, S. Tobey, V.M. Lynch, E. Anslyn, J. Am. Chem. Soc. 124 (2002) 13731.
[58] P. Molenveld, W.M.G. Stikvoort, H. Kooijman, A.L. Spek, J.F.J. Engbersen, D.N. Reinhoudt, J. Org. Chem. 64 (1999) 3896.
[59] P. Molenveld, J.F.J. Engbersen, D.N. Reinhoudt, Angew. Chem. Int. Ed. 38 (1999) 3189.
[60] M.M. Ibrahim, N. Shimomura, K. Ichikawa, M. Shiro, Inorg. Chim. Acta 313 (2001) 125.
[61] J.R. Morrow, O. Iranzo, Curr. Opin. Chem. Biol. 8 (2004) 192.
[62] A. Volbeda, A. Lahm, F. Sakiyama, D. Suck, EMBO J. 10 (1991) 1607.
[63] E. Kimura, Curr. Opin. Chem. Biol. 4 (2000) 207.
[64] J. Chin, Curr. Opin. Chem. Biol. 1 (1997) 514.
[65] R.G. Bates, M. Paabo, R.A. Robinson, J. Phys. Chem. 67 (1963) 1833.
[66] E.A. Martell, R.J. Motekaitis, The Determination and Use of Stability Constants, 2nd edVCH, New York, 1992 143.
[67] D.L. Rabenstein, S.A. Daignault, A.A. Isab, A.P. Arnold, M.M. Shoukry, J. Am. Chem. Soc. 107 (1985) 6435.
[68] M.J.A. Rainer, B.M. Rode, Inorg. Chim. Acta 93 (1984) 109.
[69] R.P. Agarwal, D.D. Perrin, J. Chem. Soc. Dalton Trans. (1975) 1045.
[70] R. Jairam, P.G. Potvin, S. Balsky, J. Chem. Soc. Perkin Trans. 2 (1999) 363.
[71] U. Herry, W. Spahl, G. Trojandt, W. Steglich, F. Thaler, R. Van Eldik, Biorg. Med. Chem. 7 (1999) 699.
[72] I. Török, T. Gajda, B. Gyurcsik, G.K. Tóth, A. Péter, J. Chem. Soc. Dalton Trans. (1998) 1205.
[73] K. Ichikawa, M.K. Uddin, K. Nakata, Chem. Lett. (1999) 115.
[74] K. Ichikawa, M. Tarnai, M.K. Uddin, K. Nakata, S. Sato, J. Inorg. Biochem. 91 (2002) 437.
[75] V. Lombardo, R. Bonomi, C. Sissi, F. Mancin, Tetrahedron 66 (2010) 2198.